PHYSICAL REVIEW C, VOLUME 65, 021303(R)

Oblate stability of $A \approx 110$ nuclei near the *r*-process path

F. R. Xu,[1,2] P. M. Walker,[1] and R. Wyss[3]
[1]*Department of Physics, University of Surrey, Guildford, Surrey GU2 7XH, United Kingdom*
[2]*Department of Technical Physics, Peking University, Beijing 100871, China*
[3]*Department of Physics, Royal Institute of Technology, Frescativägen 24, S-104 05 Stockholm, Sweden*
(Received 5 November 2001; published 18 January 2002)

Even-even $A \approx 110$ nuclei approaching the astrophysical *r*-process path have been investigated using both the cranked and the configuration-constrained shell models. The calculations show that, with increasing neutron number in the $Z \geqslant 40$ nuclides, nuclear shapes evolve from prolate, through triaxial to oblate deformations. In contrast to other regions of the nuclear chart, pronounced oblate shapes dominate the collective rotation from ground states to very high spins ($I \sim 40$), when $N \geqslant 70$. The stability of the oblate shapes is due to the simultaneous upper-shell neutron and proton Fermi surfaces, reinforced by the rotation alignment behavior of both nucleon types. Configuration-constrained calculations predict the coexistence of well-deformed prolate and oblate multiquasiparticle (isomeric) states.

DOI: 10.1103/PhysRevC.65.021303 PACS number(s): 21.60.Cs, 21.10.Re, 27.60.+j

It is rare for nuclear ground states to have oblate deformations, and recent observations of nuclides in the $A \approx 80$ and 190 regions near the proton drip line have led to renewed interest in the stability of oblate shapes [1–6]. Although coexisting oblate and prolate shapes have been observed in these proton-rich $A \approx 80$ and 190 regions, the collective rotation of the oblate structures is usually not favored energetically in competition with prolate configurations (due to a lower moment of inertia for collective oblate rotation). Also, the oblate shapes are generally soft [7,8], and they become unstable with increasing rotational spin. Perhaps the only exceptions are a few of the $A \approx 190$ mercury and platinum isotopes, where the oblate deformation, however, is very small [9]. It remains, therefore, an interesting question as to whether there exist well-deformed, oblate ground states that continue to be energetically favored under rotation.

The importance of oblate shapes is not only due to their rare occurrence and different behavior, but also there is a direct link to the properties of the nuclear mean field. A recent paper has analyzed the properties of the Nilsson potential to explain the observation that about 86% of nuclides are prolate [10]. The authors also pointed out that the proportion of prolate and oblate nuclides is sensitive to the detailed form of the potential and provides a crucial test of the strength of the spin-orbit force [10]. Since the isospin dependence of the spin-orbit force is still not well established, the observation of a region of nuclei with stable oblate shapes would form an interesting testing ground for mean-field models. From the systematics of observed rotational bands, it is clear that the filling of oblate favoring single-particle levels is not enough to result in oblate shapes. Other requirements are necessary, such as deformed shell gaps and/or rotational-alignment effects.

In this Rapid Communication, we investigate neutron-rich $A \approx 110$ nuclides, with Fermi surfaces in the upper halves of the $Z = 28-50$ and $N = 50-82$ shells, approximately $40 \leqslant Z \leqslant 46$ and $66 \leqslant N \leqslant 76$. Skalski *et al.* [11] have performed global shape calculations that already indicate oblate shapes in this $A \approx 110$ region, though with limited consideration of the triaxiality degree of freedom and limited discussion of the collective oblate rotation. We now investigate this region in more detail, including for the first time the diabatic calculation of multiquasiparticle (multi-qp) configurations.

Before presenting the detailed calculations, we also like to mention the importance of these neutron-rich $A \approx 110$ nuclides in nuclear astrophysics. These nuclides approach the *r*-process (rapid neutron capture process) path that is defined by the equilibrium between neutron capture and photodisintegration. Neutron capture terminates when the neutron separation energies are about 2 MeV, i.e., about 15–20 mass units away from the valley of stability [12]. Beta decays then drive the neutron-rich nuclei towards the line of β stability. Calculated half-lives crucially depend on mass calculations, which in turn are sensitive to the shape degrees of freedom. About half of the $A > 60$ nuclei observed in nature were produced in the *r* process. The solar elemental abundance peaks near $A = 80,130$, and 195 correspond to the neutron shell closures of $N = 50,82$, and 126, respectively. Theoretically, the modeling of astrophysical processes relies heavily on the structure knowledge of *r*-process nuclides.

Experimentally, some *r*-process nuclides can now be reached with modern facilities. Using the projectile fission of uranium at relativistic energies, for example, very neutron-rich isotopes with $N/Z \rightarrow 1.8$ in the $A \approx 110$ region, e.g., ^{110}Zr, ^{114}Mo, ^{119}Ru, and ^{124}Pd, have been identified [13]. For $40 \leqslant Z \leqslant 46$, the heaviest even-even isotopes with known excited states are ^{104}Zr [14], ^{108}Mo [15], ^{114}Ru [16], and ^{118}Pd [17]. As the nuclei become more neutron rich, experimental measurements are usually more difficult due to the lower production cross sections. In these cases, isomeric states could be of advantage, since decays from isomers can provide useful structure information. Isomerism is also important for astrophysical processes, because the existence of isomers can affect the *r* process [18]. In the present work, we focus on the theoretical understanding of extreme neutron-rich $A \approx 110$ nuclides near the *r*-process path. Both collective-rotational and multi-qp states are studied.

The nonaxial deformed Woods-Saxon (WS) potential [19] is employed. Collective rotation is investigated in the frame of the cranked shell model by means of total Routhian sur-

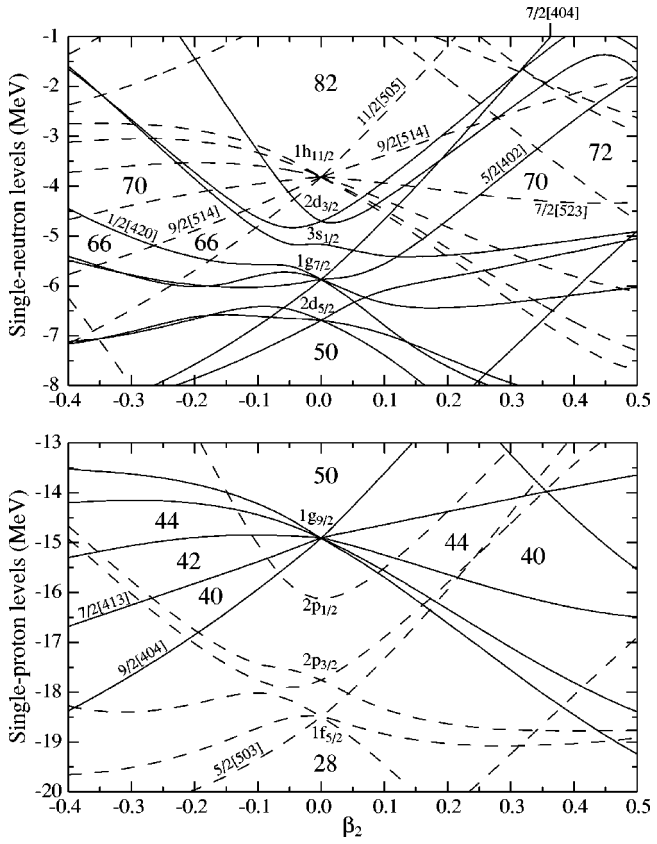

FIG. 1. The calculated single-neutron (top) and single-proton (bottom) levels of the Woods-Saxon potential. Axial symmetry is assumed with $\beta_4=-|\beta_2|/6$ which gives approximately the hexadecapole value of the ground states obtained from the TRS calculations. Positive (negative) parity is indicated by solid (dashed) lines.

face (TRS) calculations in the three-dimensional deformation space of β_2, γ, and β_4. Both monopole and double-stretched quadrupole pairings are included [22]. The monopole pairing strength G is determined by the average-gap method [20], and quadrupole pairing strengths are obtained by restoring the Galilean invariance broken by the seniority pairing force [21]. To avoid the spurious phase transition encountered in the BCS approach, we use approximate particle-number projection (Lipkin-Nogami pairing [23]). Pairing correlations are dependent on the rotational frequency (ω) and deformation. In order to include such dependence in the TRS, we have performed pairing-deformation-frequency self-consistent TRS calculations, i.e., for any given deformation and frequency, pairings are self-consistently calculated by the HFB-like method [23]. At a given frequency, the deformation of a state is determined by minimizing the calculated TRS.

Figure 1 displays the calculated single-particle levels of the Woods-Saxon potential. It can be determined that the neutrons and protons have reinforcing effects that favor oblate shapes, for the nuclides that have the neutron and proton Fermi surfaces in the upper halves of the $N=50-82$ and $Z=28-50$ shells, approximately $70\leqslant N<82$ and $40\leqslant Z<50$. We now consider the results of the shape calculations in more detail. For the $Z=40$ zirconium isotopes with $66\leqslant N\leqslant 76$, the TRS calculations show two coexisting minima, prolate with $\beta_2\approx 0.35$ and oblate around $\beta_2\approx 0.2$. (Since the shape is specified in the β_2-γ plane, the β_2 value is always positive.) When $N\geqslant 72$, oblate shapes become yrast and these oblate shapes remain stable upto very high spins ($I\sim 40$). Figure 2 (left) shows calculated TRS's for ^{112}Zr ($N=72$). For the $Z=42$ molybdenum isotopes, ^{108}Mo ($N=66$) has a γ-soft triaxial minimum around $\beta_2\approx 0.3$ and $|\gamma|\approx 20°$. With increasing rotational frequency, a collective $\gamma\approx -20°$ minimum becomes deeper, while the less-collective $\gamma\approx +20°$ minimum disappears gradually. In ^{110}Mo ($N=68$) the minimum becomes more oblate. For $N\geqslant 70$, the molybdenum isotopes have oblate minima around $\beta_2\approx 0.22$, and approaching the $N=82$ shell closure, the oblate deformations become smaller. Neutron-rich $Z=44$ ruthenium isotopes have similar deformation evolution to the molybdenum isotopes. The nuclei ^{110,112}Ru ($N=66,68$) are triaxially soft, corresponding to the observation of very low 2_2^+ γ-vibrational states around ^{112}Ru [16]. The generalized-collective-model calculations also showed the soft triaxiality [24], and Nazarewicz *et al.* [25] emphasize the importance of this region of triaxiality. Heavier ruthenium isotopes ($N\geqslant 70$), however, have oblate (or approximately oblate) shapes. As we are interested in the stable oblate shapes, two more examples, ^{112}Mo and ^{114}Ru, are also shown in Fig. 2. There are similar deformations for neutron-rich palladium isotopes. Since the palladium proton number of $Z=46$ is closer to the magic number of $Z=50$, these isotopes are in general softer in shape.

Compared to the $A\approx 80$ and 190 regions, neutron-rich $A\approx 110$ nuclei have more stable oblate shapes. We calculate that the oblate structure can stay yrast up to at least $\hbar\omega\approx 1.0$ MeV (corresponding to $I\approx 36$, see Fig. 2). The oblate minima become in general deeper (stiffer) with increasing rotational frequency. This type of rotational enhancement of oblate stability has also been calculated in the upper half of the $N=82-126$, $Z=50-82$ shell, e.g., in neutron-rich hafnium isotopes where $Z=72$ and $N\approx 110$ [26,27]. However, the hafnium isotopes have prolate ground states. Nevertheless, for high spins (approximately $I>20$) collective oblate states become lower in energy than the collective prolate states. It was found that the appearance of hafnium oblate shapes is mainly due to the rotational alignments of both the $i_{13/2}$ neutrons and the $h_{11/2}$ protons. For the $A\approx 110$ region, the Fermi surface of the $N\approx 72$ neutrons locates in the top region of the neutron $h_{11/2}$ subshell, where the Coriolis effect is strong due to the oblate low-K (or intermediate-K) high-j feature. Therefore, the oblate-favoring rotational effect should be expected. The calculations show that one pair of $h_{11/2}$ neutrons aligns at $\hbar\omega\approx 0.3$ MeV($I\approx 12$). Further, due to the corresponding location of the $Z\approx 44$ (oblate) Fermi surface, two $g_{9/2}$ protons align around $\hbar\omega\approx 0.5$ MeV. At $\hbar\omega>1.0$ MeV, $\beta_2\approx 0.45$ prolate superdeformed bands are calculated to become lower in energy, which has also been shown in Refs. [11,28]. The high-spin superdeformed states are induced by the $\nu i_{13/2}$ and $\pi h_{11/2}$ intruder orbitals.

Experimental quadrupole moments have been deduced [29] from γ-ray line-shape analysis for even-even $^{102-108}$Mo

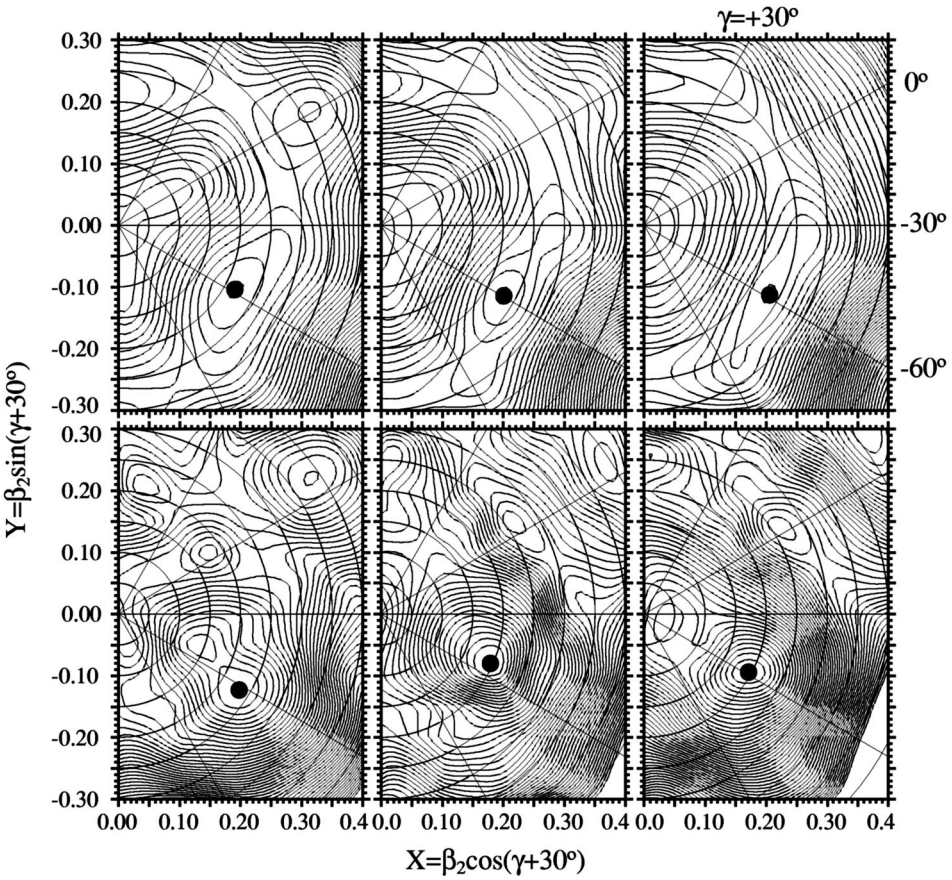

FIG. 2. Calculated total Routhian surfaces for ^{112}Zr (left), ^{112}Mo (middle), and ^{114}Ru (right). The top panel is calculated at $\hbar\omega = 0.1$ MeV (before backbendings) and the bottom panel is for $\hbar\omega = 1.0$ MeV (corresponding to $I \approx 36$). A black dot indicates the lowest minimum in each case. The $(\beta_2, \gamma, \beta_4)$ values at the minima are $(0.22, -59°, -0.04)$ and $(0.23, -62°, -0.01)$ for $\hbar\omega = 0.1$ MeV and $\hbar\omega = 1.0$ MeV, respectively, in ^{112}Zr; $(0.23, -60°, -0.05)$ and $(0.20, -54°, -0.03)$, respectively, in ^{112}Mo; and $(0.23, -59°, -0.05)$ and $(0.20, -59°, -0.03)$, respectively, in ^{114}Ru. The energy difference between neighboring contours is 200 keV.

($N = 60-66$) indicating triaxiality for rotational states at intermediate spins. This is consistent with our calculations. For $N \geqslant 68$ nuclides in this mass region, no conclusions regarding shapes have been made experimentally, though rotational bands have been observed for heavy ruthenium isotopes $^{108-114}$Ru ($N = 64-70$) [16]. As discussed above, we calculate that $^{108-112}$Ru have γ-soft triaxial deformations and ^{114}Ru is γ-soft oblate at low spins (see Fig. 2). The calculated results show also that $^{108-112}$Ru have almost the same values of bandhead moment of inertia, $J^{(1)} \approx 18\hbar^2$ MeV, and ^{114}Ru has $J^{(1)} \approx 14\hbar^2$ MeV. From the data [16], $J^{(1)} \approx 13\hbar^2$ MeV for $^{108-112}$Ru and $11\hbar^2$ MeV for ^{114}Ru. We can see a striking decrease in the $J^{(1)}$ value between $^{108-112}$Ru and ^{114}Ru in both theory and experiment. This could be a signal for the deformation change which is seen in our calculations, but additional observables are needed to establish the actual shapes.

The calculations give in general larger moments of inertia and earlier backbendings than observed experimentally. This is related to the choice of the pairing strength *G*. In our previous work [30], it was found that moments of inertia and backbendings are very sensitive to the (neutron and proton) *G* values used. In the average gap method [20], which is used in the present work, the *G* values are determined by fitting experimental odd-even mass differences with the average pairing gap. However, it has been shown that the mean field itself gives contributions to odd-even mass differences [30–33]. The inclusion of the mean-field effect can lead to a slight adjustment in the *G* values, e.g., about a $5-10\,\%$ increase in the $A \approx 180$ region [30,33]. The adjusted *G* values in that case gave improved and consistent descriptions, at the same time, for moments of inertia, backbendings, and quasiparticle excitation energies [30,33]. In the present case, a small increase in the *G* values would significantly lower theoretical moments of inertia and delay backbendings, and hence improve the agreement with experimental data. However, this kind of adjustment of the *G* values requires accurate nuclear masses. In the present work, we have not attempted to modify the *G* values, since a small *G* adjustment does not influence deformations [30,33]. In triaxial cases, e.g., in $^{108-112}$Ru, two- or three-dimensional cranking could improve the calculations further.

Isomerism can be important for both astrophysics and nuclear structure. The existence of isomeric states can affect the *r* process path [18]. In addition, isomers can provide possibilities to observe excited states of nuclei far from stability (see, for example, Ref. [34]). The configuration-constrained method [33] has been used for the potential-energy-surface (PES) calculations of multi-qp states. In this method, the orbitals involved in a given configuration are identified and diabatically blocked by calculating the average Nilsson numbers of the orbitals [33]. The shape and excitation energy of a multi-qp state can be obtained from the configuration-constrained PES. It is well known that an axial deformation and high-*K* value provide good conditions for the formation of isomeric states [35]. Experiments have observed $K^\pi = 4^-$ isomers with the configuration $\nu\frac{5}{2}[532]$

TABLE I. Calculated prolate two-quasineutron states in ^{110,112,114}Zr. Note: The configurations are $\nu\frac{7}{2}[523]\otimes\frac{5}{2}[402]$ for the 6^- states and $\nu\frac{9}{2}[514]\otimes\frac{5}{2}[402]$ for the 7^- states. For the ^{112}Zr ground state, the prolate minimum is competitive with the oblate one (see also Fig. 2). $|\gamma|$ is used since the PES is reflection symmetric about $\gamma=0°$ and $\pm 60°$ for nonrotational states.

Nuclei		Prolate multi-qp states				Ground states		
	K^π	E_{ex} (MeV)	β_2	β_4	$\|\gamma\|$	β_2	β_4	$\|\gamma\|$
^{110}Zr	6^-	1.6	0.33	−0.04	0°	0.35	−0.04	0°
^{112}Zr	6^-	1.7	0.36	−0.03	2°	0.22	−0.04	60°
^{112}Zr	7^-	2.0	0.32	−0.05	0°			
^{114}Zr	7^-	2.7	0.36	−0.04	1°	0.17	−0.04	60°

$\otimes\frac{3}{2}[411]$ in the $N=62$ isotones, ^{102}Zr [36] and ^{100}Sr [37]. The observed excitation energies are about 1.8 MeV and 1.6 MeV, respectively. Our calculations show prolate 4^- states, with $\beta_2\approx 0.35$ and $E_{ex}\approx 1.3$ MeV. The calculated energies are lower than the experimental values. This is also related to the G value, as discussed above in the calculation of moments of inertia. The excitation energy of a multi-qp state is very sensitive to the G value [33] (note that G is model dependent). About an 8% increase in the neutron G value can reproduce the energies of the observed 4^- isomers. This is also consistent with the requirement for reproducing the moments of inertia.

We have made a search for a variety of possible multi-qp states in the neutron-rich $A\approx 110$ region. In heavy molybdenum, ruthenium, and palladium isotopes, the TRS calculations show no prolate minima, and, correspondingly, no prolate multi-qp states have been found in these nuclei by performing configuration-constrained PES calculations. The $N\leqslant 76$ zirconium isotopes have prolate minima around $\beta_2\approx 0.35$ (see Fig. 2). It is also known that even-even $N=74$ isotones ($Z>50$) have systematically $\nu\frac{7}{2}[404]\otimes\frac{9}{2}[514]$, $K^\pi=8^-$ isomers with $\beta_2\approx 0.15$–0.25 prolate deformations [38]. At larger deformations, around $\beta_2\approx 0.35$, the particle-hole excitation with this 8^- configuration may be favored for $N=76-82$ (see Fig. 1). However, our configuration-constrained calculations show no prolate $\nu\frac{7}{2}[404]\otimes\frac{9}{2}[514]$ 8^- states in the $Z<50$ region. The ^{116}Zr($N=76$) nucleus has a prolate minimum that is too shallow to form the $K^\pi=8^-$ state. For $N=70-74$ (around $\beta_2\approx 0.35$) the neutron high-K orbitals, $\frac{9}{2}[514]$, $\frac{5}{2}[402]$, and $\frac{7}{2}[523]$ (see Fig. 1) are available to make high-K excitations. Table I lists calculated prolate two-quasineutron states in the $N=70-74$ zirconium isotopes. These high-K states lie less than 1 MeV above the respective yrast lines. The large axially symmetric deformations and high K values, combined with the negative parity and low energies, could result in isomerism. Figure 3 (left panel) displays the calculated PES for the $\nu\frac{9}{2}[514]\otimes\frac{5}{2}[402]$, $K^\pi=7^-$ state in ^{114}Zr.

TABLE II. Calculated oblate $\nu\frac{9}{2}[514]\otimes\frac{1}{2}[420]$, $K^\pi=5^-$ states in the $N=66$ isotones. Note: The $N=66$ isotones ($Z\leqslant 40$) have oblate 0_2^+ states at 0.6−1.5 MeV above their prolate ground states. The nuclides ^{108}Mo, ^{110}Ru, and ^{112}Pd are γ soft in both the ground states and the $K^\pi=5^-$ configurations.

Nuclei	Oblate multi-qp states				Ground states		
	E_{ex} (MeV)	β_2	β_4	$\|\gamma\|$	β_2	β_4	$\|\gamma\|$
^{100}Se	1.7	0.25	0.0	59°	0.29	−0.03	0°
^{102}Kr	2.1	0.27	0.0	60°	0.32	−0.01	0°
^{104}Sr	3.0	0.25	−0.01	60°	0.34	−0.01	0°
^{106}Zr	2.7	0.22	−0.02	63°	0.34	−0.02	0°
^{108}Mo	1.4	0.22	−0.03	63°	0.32	−0.01	18°
^{110}Ru	1.4	0.23	−0.03	65°	0.28	−0.01	23°
^{112}Pd	1.4	0.22	−0.03	65°	0.25	−0.02	40°

For oblate shapes, we have found that the $\nu\frac{9}{2}[514]\otimes\frac{1}{2}[420]$ configuration (see Fig. 1) can form well-deformed *oblate* low-energy $K^\pi=5^-$ states in the $N=66$ isotones. Table II gives the calculated information for the 5^- states, with an extension to lighter isotones. The calculated PES of the 5^- state in ^{106}Zr is also shown in Fig. 3 (right panel). Note that ^{106}Zr has a prolate ground state. It would be remarkable indeed if these excited oblate multi-qp states could be identified experimentally. The inhibition of the electromagnetic decay, on account of the shape change, in addition to the K-value change, may result in long half-lives.

In summary, the $A\approx 110$ nuclei near the r-process path have been investigated using both the cranked and the configuration-constrained shell model. It is found that, for about $N\geqslant 70$, stable oblate structure dominates the collective rotation up to $I\approx 40$. For oblate rotation, one pair of $h_{11/2}$

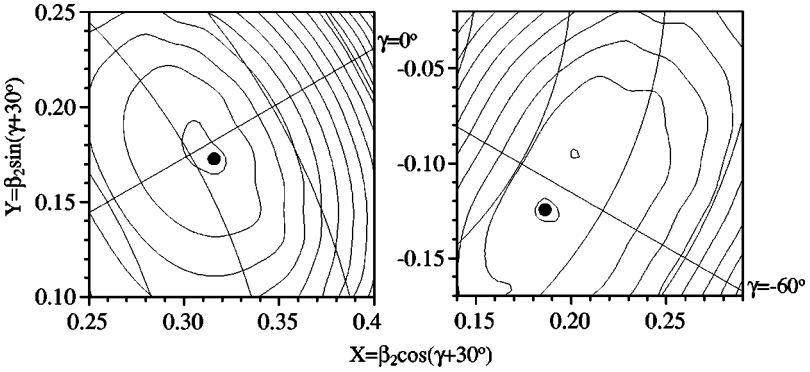

FIG. 3. Calculated configuration-constrained potential energy surfaces for the *prolate* $\nu\frac{9}{2}[514]\otimes\frac{5}{2}[402]$, $K^\pi=7^-$ state in ^{114}Zr (left) and for the *oblate* $\nu\frac{9}{2}[514]\otimes\frac{1}{2}[420]$, $K^\pi=5^-$ state in ^{106}Zr (right). The calculated deformations and excitation energies can be found in Tables I and II. Note that the scales are different from Fig. 2. The energy difference between neighboring contours is 200 keV. For these nonrotational states, the PES's are reflection symmetric about the $\gamma=0°$ and $-60°$ axes.

neutrons aligns at $\hbar\omega \approx 0.3$ MeV, and a pair of $g_{9/2}$ protons aligns at $\hbar\omega \approx 0.5$ MeV. The stability of the oblate shapes is due to the simultaneous upper-shell neutron and proton Fermi surfaces, reinforced by the rotation-alignment behavior of both nucleon types. Although, classically, the moment of inertia for an oblate shape is smaller than for a prolate shape, the specific quantum nature of the atomic nucleus results here in larger moments of inertia for oblate shapes, due to specific quasiparticle alignments. Possible low-energy prolate and oblate multi-qp states are also predicted. Negative-parity two-quasineutron states in $^{110-114}$Zr have large prolate deformations around $\beta_2 \approx 0.35$. The $\nu\frac{9}{2}[514] \otimes \frac{1}{2}[420]$, $K^\pi = 5^-$ states in the $N = 66$ isotones are oblate deformed with $\beta_2 \approx 0.25$, and, especially if isomeric, may be observable experimentally.

This work was supported by the U.K. Royal Society. F.R.X. acknowledges support from the Major State Basic Research Development Program of China (G2000077400), the Chinese Ministry of Education, and Peking University. R.W. thanks the Swedish Science Council.

[1] S.M. Fischer, D.P. Balamuth, P.A. Hausladen, C.J. Lister, M.P. Carpenter, D. Seweryniak, and J. Schwartz, Phys. Rev. Lett. **84**, 4064 (2000).
[2] C. Chandler *et al.*, Phys. Rev. C **56**, R2924 (1997).
[3] G. de Angelis *et al.*, Phys. Lett. B **415**, 217 (1997).
[4] A. Petrovici, K.W. Schmidt, and A. Faessler, Nucl. Phys. **A665**, 333 (2000).
[5] G.D. Dracoulis, A.P. Byrne, A.M. Baxter, P.M. Davidson, T. Kibédi, T.R. McGoram, R.A. Bark, and S.M. Mullins, Phys. Rev. C **60**, 014303 (1999).
[6] A.N. Andreyev *et al.*, Nature (London) **405**, 430 (2000).
[7] R. Bengtsson, T. Bengtsson, J. Dudek, G. Leander, W. Nazarewicz, and J. Zhang, Phys. Lett. B **183**, 1 (1987).
[8] W. Nazarewicz, Phys. Lett. B **305**, 195 (1993).
[9] H. Hübel, A.P. Byrne, S. Ogaza, A.E. Stuchberry, G.D. Dracoulis, and M. Guttormsen, Nucl. Phys. **A453**, 316 (1986).
[10] N. Tajima and N. Suzuki, Phys. Rev. C **64**, 037301 (2001).
[11] J. Skalski, S. Mizutori, and W. Nazarewicz, Nucl. Phys. **A617**, 282 (1997).
[12] J.J. Cowan, F.-K. Thielemann, and J.W. Truran, Phys. Rep. **208**, 267 (1991).
[13] M. Bernas *et al.*, Phys. Lett. B **415**, 111 (1997).
[14] M.A.C. Hotchkis *et al.*, Phys. Rev. Lett. **64**, 3123 (1990).
[15] M.A.C. Hotchkis *et al.*, Nucl. Phys. **A530**, 111 (1991).
[16] J.A. Shannon *et al.*, Phys. Lett. B **336**, 136 (1994); Q.H. Lu *et al.*, Phys. Rev. C **52**, 1348 (1995).
[17] X.Q. Zhang *et al.*, Phys. Rev. C **63**, 027302 (2001).
[18] G. Martinez-Pinedo and K. Langanke, Phys. Rev. Lett. **83**, 4502 (1999).
[19] W. Nazarewicz, J. Dudek, R. Bengtsson, T. Bengtsson, and I. Ragnarsson, Nucl. Phys. **A435**, 397 (1985).
[20] P. Möller and J.R. Nix, Nucl. Phys. **A536**, 20 (1992).
[21] H. Sakamoto and T. Kishimoto, Phys. Lett. B **245**, 321 (1990).
[22] W. Satuła and R. Wyss, Phys. Rev. C **50**, 2888 (1994); Phys. Scr. **T56**, 159 (1995).
[23] W. Satuła, R. Wyss, and P. Magierski, Nucl. Phys. **A578**, 45 (1994).
[24] D. Troltenier, J.P. Draayer, B.R.S. Babu, J.H. Hamilton, A.V. Ramayya, and V.E. Oberacker, Nucl. Phys. **A601**, 56 (1996).
[25] W. Nazarewicz, J. Dobaczewski, M. Matev, S. Mizutori, and W. Satuła, Acta Phys. Pol. B **32**, 2349 (2001).
[26] R.R. Hilton and H.J. Mang, Phys. Rev. Lett. **43**, 1979 (1979).
[27] F.R. Xu, P.M. Walker, and R. Wyss, Phys. Rev. C **62**, 014301 (2000).
[28] R.R. Chasman, Phys. Rev. C **64**, 024311 (2001).
[29] A.G. Smith *et al.*, Phys. Rev. Lett. **77**, 1711 (1996).
[30] F.R. Xu, R. Wyss, and P.M. Walker, Phys. Rev. C **60**, 051301(R) (1999).
[31] W. Satuła, J. Dobaczewski, and W. Nazarewicz, Phys. Rev. Lett. **81**, 3599 (1998).
[32] K. Rutz, M. Bender, P.-G. Reinhard, and J.A. Maruhn, Phys. Lett. B **468**, 1 (1999).
[33] F.R. Xu, P.M. Walker, J.A. Sheikh, and R. Wyss, Phys. Lett. B **435**, 257 (1998).
[34] Zs. Podolyak *et al.*, Phys. Lett. B **491**, 225 (2000); M.N. Mineva *et al.*, Eur. Phys. J. A **11**, 9 (2001).
[35] P.M. Walker and G.D. Dracoulis, Nature (London) **399**, 35 (1999).
[36] J.L. Durell *et al.*, Phys. Rev. C **52**, R2306 (1995).
[37] B. Pfeiffer *et al.*, Z. Phys. A **353**, 1 (1995).
[38] F.R. Xu, P.M. Walker, and R. Wyss, Phys. Rev. C **59**, 731 (1999).